Journal of Biomechanics 85 (2019) 164–172

Contents lists available at ScienceDirect

Journal of Biomechanics

journal homepage: www.elsevier.com/locate/jbiomech
www.JBiomech.com

Statistical shape modelling versus linear scaling: Effects on predictions of hip joint centre location and muscle moment arms in people with hip osteoarthritis

Jasvir S. Bahl [a,*], Ju Zhang [b], Bryce A. Killen [c], Mark Taylor [d], Lucian B. Solomon [e,f], John B. Arnold [a], David G. Lloyd [c], Thor F. Besier [b,g], Dominic Thewlis [f]

[a] Alliance for Research in Exercise, Nutrition and Activity (ARENA), Sansom Institute for Health Research & School of Health Sciences, University of South Australia, Adelaide, Australia
[b] Auckland Bioengineering Institute, University of Auckland, Auckland, New Zealand
[c] Gold Coast Centre for Orthopaedics Research, Engineering and Education (GCORE), Menzies Health Institute Queensland, Griffith University, Australia
[d] The Medical Device Research Institute, College of Science and Engineering, Flinders University, Adelaide, South Australia, Australia
[e] Department of Orthopaedics and Trauma, Royal Adelaide Hospital, Port Road, Adelaide, South Australia, Australia
[f] Centre for Orthopaedic and Trauma Research, Discipline of Orthopaedics and Trauma, University of Adelaide, Adelaide, South Australia, Australia
[g] Department of Engineering Science, Faculty of Engineering, University of Auckland, Auckland, New Zealand

ARTICLE INFO

Article history:
Accepted 16 January 2019

Keywords:
Hip joint centre
Statistical shape model
Musculoskeletal modelling
Scaling

ABSTRACT

Marker-based dynamic functional or regression methods are used to compute joint centre locations that can be used to improve linear scaling of the pelvis in musculoskeletal models, although large errors have been reported using these methods. This study aimed to investigate if statistical shape models could improve prediction of the hip joint centre (HJC) location. The inclusion of complete pelvis imaging data from computed tomography (CT) was also explored to determine if free-form deformation techniques could further improve HJC estimates. Mean Euclidean distance errors were calculated between HJC from CT and estimates from shape modelling methods, and functional- and regression-based linear scaling approaches. The HJC of a generic musculoskeletal model was also perturbed to compute the root-mean squared error (RMSE) of the hip muscle moment arms between the reference HJC obtained from CT and the different scaling methods. Shape modelling without medical imaging data significantly reduced HJC location error estimates (11.4 ± 3.3 mm) compared to functional (36.9 ± 17.5 mm, p = <0.001) and regression (31.2 ± 15 mm, p = <0.001) methods. The addition of complete pelvis imaging data to the shape modelling workflow further reduced HJC error estimates compared to no imaging (6.6 ± 3.1 mm, p = 0.002). Average RMSE were greatest for the hip flexor and extensor muscle groups using the functional (16.71 mm and 8.87 mm respectively) and regression methods (16.15 mm and 9.97 mm respectively). The effects on moment-arms were less substantial for the shape modelling methods, ranging from 0.05 to 3.2 mm. Shape modelling methods improved HJC location and muscle moment-arm estimates compared to linear scaling of musculoskeletal models in patients with hip osteoarthritis.

1. Introduction

Musculoskeletal models enable a better understanding of physiological variables such as muscle forces and internal joint loads that are generally not measurable experimentally. However, the predictive power and application of computational models as clinical tools are limited, partly from the difficulty of generating models that capture individualised variations in the musculoskeletal anatomy and physiology (Hicks et al., 2015; Seth et al., 2011). These issues can cause inaccurate simulations of muscle and joint forces (Gerus et al., 2013; Lerner et al., 2015).

Typically, musculoskeletal models are personalised by simple linear scaling of segment anthropometries from a generic musculoskeletal model (Kainz et al., 2017c). Individual segment dimensions can be determined using surface anatomical landmarks alone (O'Connor et al., 2018) or together with derived hip joint centre (HJC) locations (Kainz et al., 2017c). Inclusion of HJC locations in the scaling process has been shown to result in more precise

* Corresponding author at: Alliance for Research in Exercise, Nutrition and Activity (ARENA), Sansom Institute for Health Research, University of South Australia, University of South Australia, City East Campus, Adelaide, SA 5001, Australia.
E-mail address: jasvir.bahl@mymail.unisa.edu.au (J.S. Bahl).

https://doi.org/10.1016/j.jbiomech.2019.01.031
0021-9290/

estimates of pelvis dimensions compared to using surface anatomical markers alone (Kainz et al., 2017c). Hip joint centre (HJC) locations should be estimated using either functional joint centre estimation methods in people with sufficient hip range of motion (ROM) (Piazza et al., 2001; Wu et al., 2002) or Harrington's regression equation for subjects with limited hip ROM (Kainz et al., 2015). Both functional- and regression-based approaches demonstrate average HJC location errors of 20–30 mm (Bell et al., 1989; Davis et al., 1991; Harrington et al., 2007). Errors from regression equations stem from a combination of marker placement error and limitations of the regression equation in approximating the true variation in the population (Schwartz and Rozumalski, 2005), whilst errors from functional methods stem from limited ROM, functional trial performance and soft tissue artefact (Fiorentino et al., 2017; Kainz et al., 2017b; Piazza et al., 2001). Consequently, these methods are not appropriate for individuals who are obese, have hip pain or are elderly. Patients with hip pathology, such as osteoarthritis, may be affected by the aforementioned limitations, reducing the applicability of functional- and regression-based methods in estimating HJC location in this population (Flugsrud et al., 2006; Zeni et al., 2015).

Atlas-based statistical shape modelling ('shape modelling') may provide a solution to more accurately capture the anatomical and geometrical variations of the musculoskeletal system (Zhang et al., 2016, 2014b). Using this approach, a shape model containing a mean mesh and principal components trained on a large sample of medical imaging data can be used to reconstruct musculoskeletal geometry from optical motion capture data ('PCFit') (Zhang et al., 2014b). Imaging data from CT can be also incorporated into the shape modelling workflow, using free-form deformation techniques to further minimise the surface-surface root-mean squared error (RMSE) (Fernandez et al., 2012), thereby ultimately improving estimations of HJC locations. While these methods have demonstrated the utility of shape models in reconstructing musculoskeletal geometry, the ability for shape modelling techniques to estimate HJC locations and muscle moment-arms, compared to linear scaling are yet to be determined.

This study aimed to examine the accuracy of HJC estimation in patients with hip osteoarthritis. Specifically, we compared shape modelling, using motion capture markers with and without CT imaging data, to the functional- and regression-based linear scaling methods. It was hypothesised that shape modelling would produce closer estimations of HJC location compared to the linear scaling methods, with reference to the HJC obtained from CT.

2. Materials and methods

The HJC locations from the shape modelling, functional and regression methods were used to adjust the HJC location of a validated lower-limb musculoskeletal model in OpenSim (gait2392) (Delp et al., 2007, 1990) to demonstrate the effect of inaccurate HJC estimation on muscle moment-arms. To this end, four scaling methods were evaluated:

1. Shape modelling + PC fit: An atlas-based approach that scaled mean meshes along PCs using only motion capture markers.
2. Shape modelling + complete CT: Integration of complete pelvis medical imaging from CT and shape modelling using free-form deformation techniques.
3. Linear scaling + functional virtual markers: Virtual HJC markers computed from the functional trial (Ehrig et al., 2011) and surface anatomical landmarks were used to scale the pelvis.
4. Linear scaling + regression virtual markers: Virtual HJC markers using a regression method (Harrington et al., 2007) and surface anatomical landmarks were used to scale the pelvis.

2.1. Participants

Fifteen subjects with hip osteoarthritis awaiting surgery for primary total hip arthroplasty participated in this study (10 male, 5 female; mean age: 67.6 ± 11 years, mean height: 1.67 ± 0.09 m, BMI: 28.86 ± 5 kg/m^2). The Central Adelaide Health Network Human Research Ethics Committee (CALHN-HREC, R20160807) approved all study procedures. All subjects provided informed written consent.

2.2. Motion capture experiment

One investigator (JB) placed 12 surface markers (14 mm diameter) on anatomical landmarks of the pelvis and lower limbs (Kainz et al., 2017a). Additionally, a cluster of four markers was strapped to each thigh and shank (Lerner et al., 2014). A static trial was captured to measure the surface landmark positions, followed by two dynamic trials (one for each hip), where the participants were instructed to complete a pre-defined StarArc pattern motion that included hip flexion-extension, hip abduction-adduction and circumduction (Camomilla et al., 2006). Marker trajectories were recorded using 10 Vicon V5 cameras (Vicon Motion Systems, Oxford, UK) at 100 Hz.

2.3. Computed tomography (CT) scan acquisition

CT images of the full pelvis were obtained from each participant in a supine position using a dual-energy Siemens SOMATOM Definition Flash (Siemens, Erlangen, Germany). The 3D geometry of each participant's pelvis was segmented using a semi-automatic threshold-based approach in the ScanIP module (version 5.0, Simpleware, UK). A recursive Gaussian filter was applied to smooth the reconstructed 3D surface model. The target model was decimated to 15,000 faces to minimise computational demands whilst retaining geometric fidelity.

2.4. Shape modelling + PC fit

The Musculoskeletal Atlas Project Client (MAPClient) containing shape models of the pelvis and lower limbs was used for morphing individualised meshes for each subject (Zhang et al., 2014b). The MAPClient is an open-source application used to build workflows to generate subject-specific musculoskeletal models using a shape model. An articulated shape model comprising the pelvis, left and right femurs, tibias, fibulas and patellae was registered to anatomical landmarks collected from the experimental motion capture trial (Fig. 1.1). Registration consisted of rigid-body translation, rotation and deformation along PCs to capture each participant's bone shape and size (Zhang et al., 2016, 2014a). Matching of the embedded landmarks on the shape model to the experimental landmarks were initially adjusted along the first PC to encourage model pose and size estimation. This was followed by iterative fitting up to five PCs to fine tune bone shape (Zhang et al., 2014b). The relative orientation of the bones was controlled by a six degrees-of-freedom (DOF) ground-pelvis joint, two three-rotational DOF spherical hip joints, and two one-rotational DOF (flexion-extension) knee joints. The pose of the model was set by registering embedded anatomical landmarks on the pelvis, femurs and tibias to the corresponding experimental landmarks.

2.5. Shape modelling + medical imaging

The *shape modelling + PC fit* pelvic mesh from each participant's motion capture data (Fig. 1.1), was further morphed to the segmented pelvis surface from the CT data (Fig. 1.2–1.4). This com-

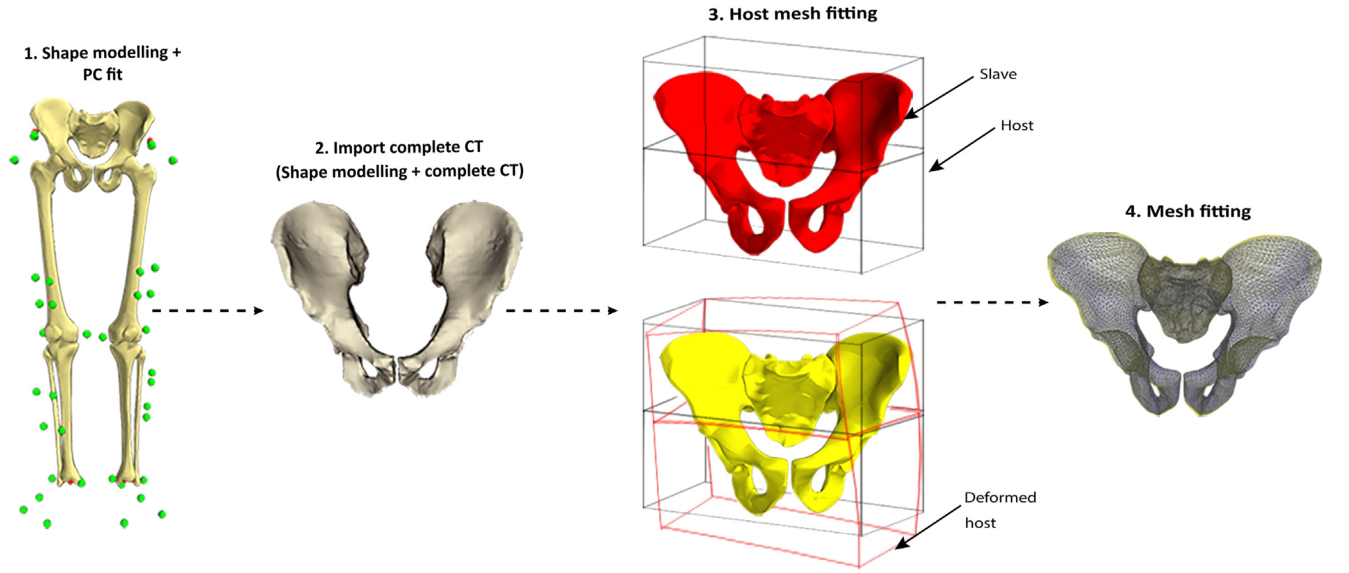

Fig. 1. Major steps of the shape modelling workflow. 1.1: The shape model and PC fit method is a one-step process to register an articulated shape model of the lower limb to the experimental marker positions from motion capture data. 1.2: The complete segmented pelvis from CT is imported into the workflow as a point-cloud. During this step the pelvis of the registered articulated shape model is discretised into a point-cloud and registered to the segmented CT data using an iterative closest point algorithm. 1.3: The registered point-cloud and atlas mesh are passed to the host mesh fit and fine mesh fit steps (1.4) where the mesh is fitted to the segmented data. The end product is a subject-specific pelvis reconstructed from motion capture data and pelvis CT.

prised of a rigid-body registration using iterative closest point to coarsely align the morphed pelvis mesh to target segmented pelvis (Besl and McKay, 1992). Following this, host mesh fitting was performed (Fig. 1.3), which consisted of a coarse non-rigid morphing of the pelvis mesh to the target point cloud, i.e. the segmented pelvis surface (Fernandez et al., 2004). Deformations of the pelvis mesh were constrained by a host mesh to reduce the degrees of freedom and penalise high deformations of the pelvis mesh to target point cloud to maintain mesh integrity. An iterative least-squares optimisation minimised the distances between the pelvis mesh and target by adjusting the control points of the host mesh. Three iterations of the host mesh fit were performed to minimise the RMS error between the source and target points. Lastly, a fine-scale fitting (Fig. 1.4) of the pelvic mesh was performed, which removed the constraint of the host mesh and allowed independent adjustment of the pelvis mesh control points (nodes) to further reduce the RMS distance between the pelvis mesh and target points.

2.6. Linear scaling methods

We used the open-source gait2392 model consisting of 23-degrees-of-freedom and 92 musculotendon actuators to represent 76 muscles in the lower extremities and torso (Delp et al., 1990). Virtual markers were placed on the OpenSim model to correspond with the experimental surface landmarks from the motion capture trials. Prior to scaling the pelvis in OpenSim, additional virtual markers were computed from the experimental motion capture data to enable the pelvis to be linearly scaled in three orthogonal directions (Fig. 2) (Kainz et al., 2017c). Scale factors were computed based on the ratio between experimental and virtual markers on the model. Two methods were used to compute the HJC

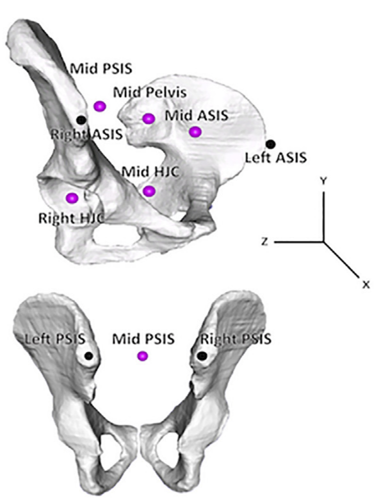

Virtual markers	
Mid ASIS	Mid-point between left and right ASIS
Mid PSIS	Mid-point between left and right PSIS
Mid Pelvis	Mid-point between Mid ASIS and MID PSIS
Mid HJC	Mid-point between left and right HJCs computed from the functional trials or the Harrington regression method
Scaling definitions	
Pelvis depth (x)	Scale factor computed using distance between Mid PSIS and Mid ASIS
Pelvis height (y)	Scale factor computed using distance between Mid Pelvis and Mid HJC
Pelvis height (z)	Scale factor computed using distance between Left and Right HJCs

Fig. 2. Experimental reflective markers (black) placed on the surface of the skin to represent the underlying anatomical landmarks of anterior superior iliac spines (ASIS) and posterior superior iliac spines (PSIS). Virtual markers (pink) were imputed as distances from the experimental markers. The HJC virtual markers were computed for the functional method and Harrington's regression method per subject. Definitions used to scale the pelvis of the gait2392 model in OpenSim are presented. (For interpretation of the references to color in this figure legend, the reader is referred to the web version of this article.)

marker: the functional method from the StarArc pattern using the Symmetric Centre of Rotation Estimation (SCoRE) (Ehrig et al., 2011) and regression equation of Harrington et al. (2007). Two models were linearly scaled for each subject in OpenSim using the predicted HJC virtual markers from the two methods.

2.7. Hip joint centre location and estimations

The reference HJC was defined as the centre of a sphere least-squares-fitted to the segmented acetabulum derived from the CT scans. Due to likely variations in acetabulum rim topography, congruency was evaluated as the RMS distance between the fit sphere and the acetabulum surface. The RMS distance, a measure of how accurately the acetabulum related to the sphere, was 1.65 ± 0.48 mm. The coordinates of the anterior superior iliac spines (ASIS), posterior superior iliac spines (PSIS) and pubic symphysis (PS) on the segmented pelvis were manually identified using a custom picker application written in Python (Version 2.7). The landmarks were used to align the model to the ISB recommended pelvis anatomical coordinate system, in which the coordinates of the reference HJC were obtained for each scaling method. The OpenSim pelvis models were rotated to align with the ISB recommended pelvis anatomical coordinate system and correct for the zero pelvic tilt in neutral for the gait2392 model. The pelvis was rotated anteriorly using a horizontal plane between the ASIS and PSIS markers, where the degree of pelvic tilt was derived from the reference model of each subject.

The HJC of the shape model was calculated as the centre of a least-squares sphere-fit to the acetabular vertices of the shape model mesh. The acetabular vertices are manually defined on the mean mesh, which stay in the acetabular region as the mean mesh is deformed during PC fitting. The HJC locations for the reference, shape models and linear scaling methods were expressed in the local pelvis coordinate system located at the mid-point of a line connecting the two anterior superior iliac spines. The HJC error was computed as the Euclidean mean distance between each scaling/morphing method's HJC and the reference HJC from the segmented pelvis.

2.8. Moment arm length

The effects of HJC location estimation error on the moment arms of the main hip muscles were analysed using the OpenSim Gait2392 model (Sherman et al., 2013). Muscles included the hip flexors (iliacus, psoas, and rectus femoris), extensors (gluteus maximus1 [superior], gluteus maximus2 [middle], and gluteus maximus3 [inferior]), and abductors (gluteus medius1 [anterior], gluteus medius2 [middle], and gluteus medius3 [posterior]). To illustrate the potential effect on moment arm lengths, the HJC of the generic OpenSim2392 gait model was adjusted in three directions based on the outputs from the linear scaling and shape modelling methods. This approach was implemented to maintain consistency and minimise the confounding effect of re-mapping muscle attachment sites and pathways to the shape model. Moment arms were computed over a typical range of hip motion reported for level walking (Winter, 1989).

2.9. Statistical analysis

Comparison of the mean HJC error from the shape model and linear scaling methods were analysed using a repeated measures analysis of variance with the repeated measure being the scaling/morphing method. Individual differences in means between the five methods were evaluated with Tukey *post hoc* comparisons. Where data violated the assumptions of equal variance for each test (determined by Levene's test) Welch's correction for unequal variance with Games-Howell *post hoc* was applied. Statistical significance was considered for $p < 0.05$. To determine the effect of HJC location estimation on moment arms, the RMSE was calculated between the reference HJC obtained from CT and each scaling method. Linear regression was used to explore the association between BMI and HJC error for each method.

3. Results

Average hip ROM for the functional trials was: flexion 25 ± 14°, extension 7 ± 10°, adduction 4 ± 5° and abduction 14 ± 7°. Compared to the two linear scaling methods, the shape model scaling methods resulted in significantly lower HJC location errors (Figs. 3 and 4, Table 1) ($p = <0.001$). Of the shape model methods, the HJC prediction errors from the shape model + complete CT were lowest, and significantly less than from the shape model + PC fit method (6.6 ± 3.1 mm and 11.4 ± 3.3 mm respectively, $p = 0.002$). There was no significant difference between linear scaling methods (functional 36.9 ± 17 mm, regression 31.2 ± 15 mm, $p = 0.11$).

There was a significant positive relationship between BMI and HJCs from the linear scaling regression ($R^2 = 0.30$, $p = 0.03$) and functional methods ($R^2 = 0.30$, $p = 0.04$). No significant associations were observed for the shape modelling methods using complete CT ($R^2 = 0.03$, $p = 0.574$) and PC fit methods ($R^2 = 0.15$, $p = 0.153$, Fig. 5).

The estimated muscles moment arms from the shape model scaling methods were similar to each other and the reference HJC, while linear scaling methods each had similar moment arms but quite different to shape model methods and reference HJC (Fig. 6 and Table 2). The shape model + complete CT models estimated moment arms (flexor, extensor, abductor) with the lowest average RMS errors compared to the reference HJC musculoskeletal model (0.49 mm, 0.41 mm, 0.18 mm), while the shape model + PC fit (2.54 mm, 1.9 mm, 0.45 mm) had marginally larger average RMS errors (Fig. 6 and Table 2). Compared to the shape model methods, the functional and regression scaling methods produced larger RMS errors for the flexor group (16.71 mm and 16.15 mm respectively), the extensor group (8.87 mm and 9.97 mm respectively) and the abductor muscle group (1.65 mm and 1.67 mm respectively).

The anterior, superior and medial displacement of the HJC using the shape modelling methods reduced the average moment arm lengths of the hip flexor muscle group (0.49 mm and 2.54 mm respectively) and hip extensor muscle group (0.41 mm and 1.9 mm respectively). The posterior, inferior and lateral HJC displacements using the linear scaling methods increased the average moment arms of the hip flexor muscle group (16.71 mm and 16.15 mm respectively) and hip extensor muscle group (8.87 mm and 9.97 mm respectively).

4. Discussion

This study's purpose was to investigate if shape modelling, with the inclusion or absence of medical imaging, could accurately predict the location of the HJC for musculoskeletal models, and thereby provide a solution to the large errors observed using current functional- and regression-based linear scaling methods. It was demonstrated that shape modelling methods produced substantially closer estimations of HJC location compared with both linear scaling methods. HJC estimations were significantly improved when complete medical imaging of the pelvis was integrated in the shape modelling workflow compared to using PCs alone to transform a lower-limb shape model. The shape modelling methods produced musculoskeletal models that estimated muscle

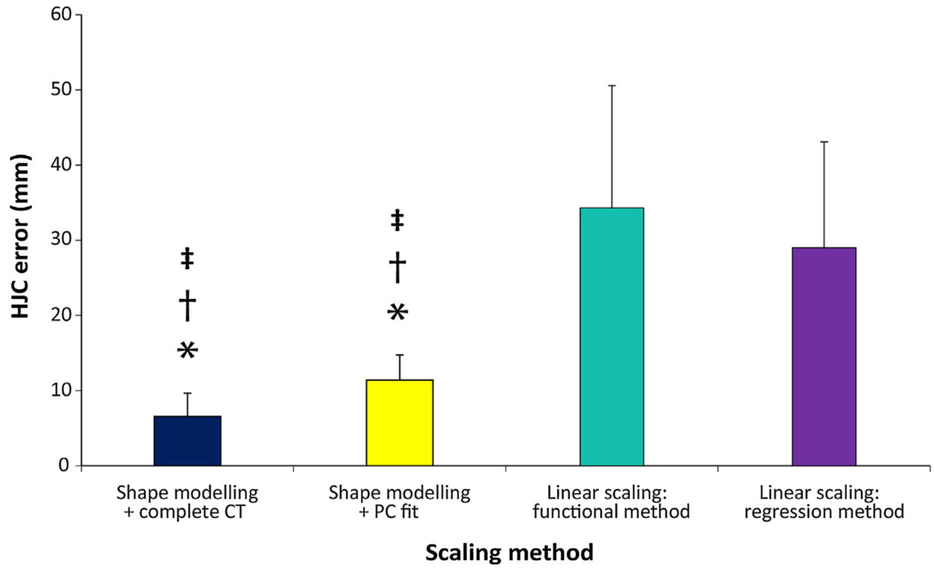

Fig. 3. Average Euclidean mean distance of the HJC using the shape modelling and linear scaling methods in relation to the reference HJC obtained from CT. *Significant difference compared to the functional method with virtual markers ($p < 0.05$). †Significant difference compared to the regression method with virtual markers ($p < 0.05$). ‡Significant difference between SSM methods ($p < 0.05$).

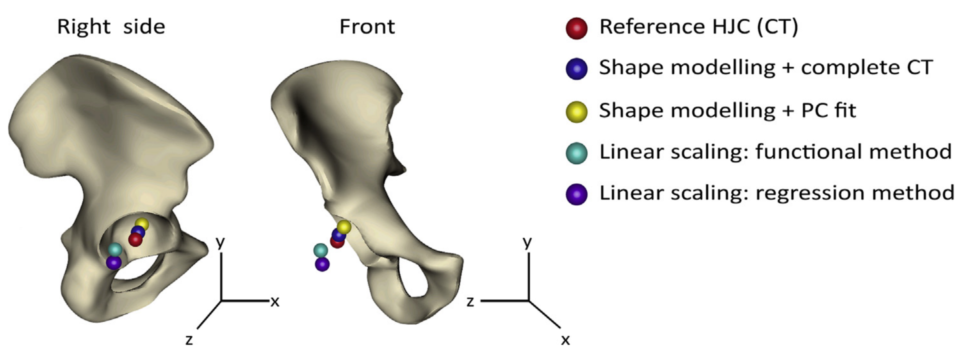

Fig. 4. Illustration of the mean hip joint centre estimates from the shape modelling and linear scaling methods compared to the CT-derived reference hip joint centre. Table 2 specifies the magnitude of the HJC errors for each method.

Table 1
Hip joint centre errors using the statistical shape modelling and conventional OpenSim linear scaling methods.

Scaling method	Euclidean mean difference (mm)	x (mm)	y (mm)	z (mm)
		+ve = anterior	+ve superior	+ve = lateral
		−ve = posterior	−ve − inferior	−ve = medial
Shape modelling + complete CT	6.6 (3.1)	1.5 (4.9)	2.9 (3.8)	−1.0 (2.1)
Shape modelling + PC fit	11.4 (3.3)	2.9 (6.4)	5.3 (5.9)	−4.3 (4.0)
Linear scaling: functional method	36.85 (17.49)	−21.3 (10.7)	−7.6 (28.9)	11.0 (11.6)
Linear scaling: regression method	31.16 (15.14)	−21.3 (12.3)	−17.7 (11.4)	9.7 (10.2)

Values are presented as mean (SD).

moments similar to the reference HJC models, while linear scaling methods produced large errors in estimated moment arms.

Shape modelling with motion capture markers (Shape modelling + PC fit) improved HJC location estimation errors up to 20 mm compared to the regression method and up to 25 mm compared to the functional method. Incorporating medical imaging with shape modelling further reduced HJC error from the linear scaling techniques to a Euclidean mean error of 7 mm with reference to the HJC obtained from CT. The larger errors observed for the functional method can be explained by the lower hip range of motion in extension, adduction and abduction compared to the recommended ROM for computing functional hip joint centres (30° of flexion/extension/abduction/adduction) (Piazza et al., 2004).

In this study of people with hip osteoarthritis and a high BMI, HJC errors of approximately 37 mm and 31 mm were found using the functional- and regression-based linear scaling methods respectively, which are substantially greater errors than those previously reported (Kainz et al., 2015). BMI explained 30% of the variation in HJC location error using the functional- and regression-based scaling methods, although further studies with a larger sample are required to verify this relationship. Nevertheless,

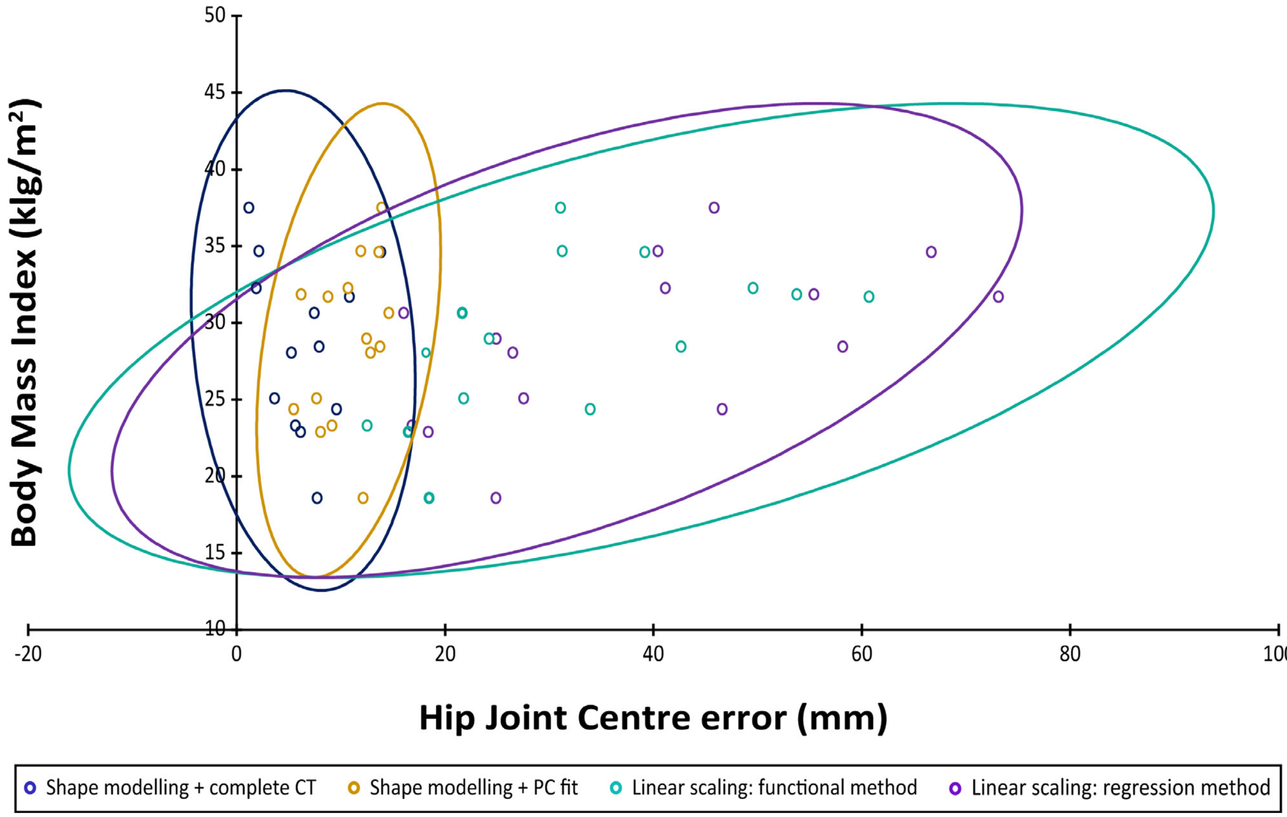

Fig. 5. Hip joint centre errors with 95% confidence ellipses using shape modelling and linear scaling methods.

these results suggest that errors for both linear scaling methods may be associated with experimenter difficulties in palpating surface landmarks to define underlying bone surfaces (Della Croce et al., 1999).

Our study demonstrates that using conventional scaling HJC estimations to linearly scale the pelvis in musculoskeletal models are not suitable for patients with larger BMI and limited hip ROM. This was observed with the effects of using the large HJC erroneous displacements, from the generic scaling methods, on the moment-arms of the hip muscles. Errors of this magnitude are large enough to substantially affect the hip muscle moment arms, resulting in erroneous results in subsequent estimation of muscle and joint contact forces (Delp and Maloney, 1993; Kirkwood et al., 1999; Lenaerts et al., 2009). The anterior, superior and medial displacement of the HJC using the shape modelling methods had minimal effect on the moment-arm of the hip abductor muscle groups. The displacement of the HJC in each direction might be inconsequential (<7 mm) to affect estimations of muscle forces and joint contact forces, with Delp and Maloney (1993) previously demonstrating errors up to 20 mm have a significant impact on the moment-and force-generating capacity of the hip abductors.

The hip flexor moment-arms were most affected by the superior and anterior displacement of the HJC estimated using the shape model with PC fit method. However, this effect was small, since errors of up to 20 mm in the superior direction can decrease hip flexor moment arm by 6% and flexion force by 27% (Delp and Maloney, 1993), whereas in the current study a 5 mm displacement was observed superiorly for the shape model with PC fit method. The HJC estimation error from the shape model with complete CT had minimal effect on all the major hip muscles demonstrating <0.8 mm RMS error compared to the reference HJC.

While there are novel findings in this study, we must identify the limitations of the work to contextualise our conclusions. First, reliability of marker placement to anatomical landmarks was not investigated in this study. However, a large margin of error can be expected with intra-examiner precision ranging from 6 to 21 mm (Della Croce et al., 1999), providing a further justification for the need to reduce the reliance on accurate placement of anatomical markers to predict HJC locations. Second, implementation of the least squares sphere fit method to obtain the reference HJC assumed sphericity of the acetabulum. However, despite good fit between sphere geometry to the CT acetabulum, variations in acetabulum topography were observed in patients with hip osteoarthritis. Other geometric shapes such as an ellipsoid may provide better templates for acetabulum shape. Third, the superior method of geometric sphere fitting to calculate the functional joint centre (Besier et al., 2003) was not used in this study. The functional SCoRE method to predict the HJC has previously demonstrated HJC estimation errors ranging from 17 to 35 mm in patients with limited him ROM (Sangeux et al., 2014). In this study, the functional HJCs from the SCoRE method resulted in larger average HJC estimation errors (36.9 ± 17.5 mm). Importantly, even if expected improvements of 5–10 mm (Sangeux et al., 2011, 2014) in HJC estimations using the geometric sphere fit method was applied to this study, erroneous predictions of the HJC location would remain. The shape modelling methods in this study were at least a quarter of the average functional HJC errors in this study with a smaller standard deviation, resulting in a reproducible method to scale musculoskeletal models. Finally, the training set of lower limb-shape models used in this study was performed on adults with no musculoskeletal abnormalities. Therefore, the application of the findings from this study cannot be applied to children or subjects with other lower limb malalignment.

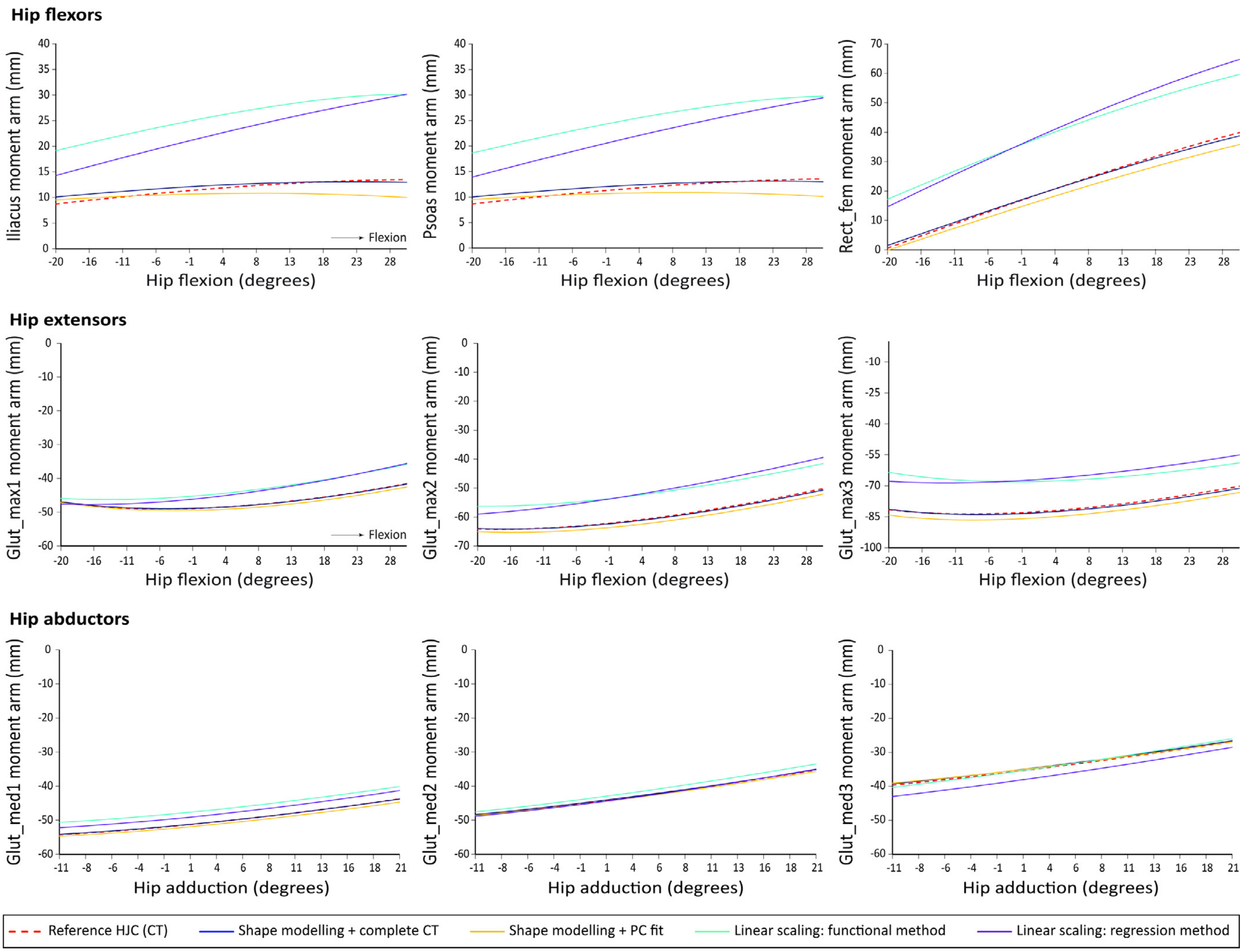

Fig. 6. Hip moment arm lengths for a sub-group of hip flexor (top row), hip extensor (middle row) and hip abductor (bottom row) muscles following adjustment of the HJC location estimated from the individual's segmented CT, shape modelling and linear scaling methods.

Table 2
Root-mean squared error (RMSE) of the moment arms between the reference HJC obtained from CT and the shape modelling and linear scaling methods.

	Shape modelling + complete CT (mm)	Shape modelling + PC fit (mm)	Linear scaling: functional method (mm)	Linear scaling regression method (mm)
Hip flexors				
Iliacus	0.42	2.24	15.51	13.34
Psoas	0.42	2.18	14.95	12.73
RecFem	0.62	3.20	19.67	22.37
Hip extensors				
GlutMax1	0.08	0.84	4.85	4.61
GlutMax2	0.37	1.72	8.63	9.77
GlutMax3	0.77	3.00	13.13	15.54
Hip abductors				
GlutMed1	0.05	0.73	3.05	2.22
GlutMed2	0.12	0.29	1.37	0.23
GlutMed3	0.38	0.34	0.53	2.55

5. Conclusion

The use of shape modelling significantly reduced the error of HJC estimation compared to the functional and regression-based methods to scale the pelvis using musculoskeletal models. In the absence of medical imaging, the use of a shape model can improve HJC mean error from 20–25 mm to 11 mm when compared to the CT-derived reference HJC. The inclusion of complete medical imaging in the shape modelling workflow further improves HJC estimation with a mean difference of 6–10 mm compared to the reference

HJC, improving on current methods by 25–30 mm. The improved accuracy and consistency from shape modelling suggest that these methods should be used in preference to linear scaling methods to generate individualised musculoskeletal models of the pelvis.

Acknowledgements

This research was supported by the Australian Government Research Training Program Scholarship for Mr Jasvir S. Bahl. JBA is currently supported by a National Health & Medical Research Council Early Career Research Fellowship (ID: 1120560). DT is currently supported by a National Health & Medical Research Council Career Development Fellowship (ID: 1126229).

Contributions

JSB, TFB and DT were responsible for the conception and design of the research. JZ and BAK assisted JSB in writing the code to process the data. MT and DGL were responsible for design of the research, interpretation of the results and revision of the manuscript. JBA and LBS were responsible for design of the research, interpretation of the results and revision of the article for important intellectual content. All authors read and approved the final version of the manuscript.

Conflicts of interest

None of the funding sources listed below had input into the study design, analysis and interpretation of the data; in the writing of the manuscript, and in the decision to submit the manuscript for publication.

Jasvir S. Bahl – No conflicts of interest to declare.

JSB is supported through an Australian Government Research Training Program Scholarship.

Bryce A. Killen – No conflicts of interest to declare.

BAK is supported by a Griffith University Postgraduate Research Scholarship.

Ju Zhang – No conflicts of interest to declare.

Mark Taylor – No conflicts of interest to declare.

Lucian B. Solomon – Institutional support from NHMRC, Royal Adelaide Hospital (RAH) research foundation, Zimmer Biomet and DePuy Johnson and Johnson.

John B. Arnold – No conflicts of interest to declare.

JBA is currently supported by a National Health & Medical Research Council Early Career Fellowship (ID: 1120560).

Thor F. Besier - No conflicts of interest to declare.

David G. Lloyd - No conflicts of interest to declare.

Dominic Thewlis – No conflicts of interest to declare. DT is the recipient of an NHMRC Career Development Fellowship (ID: 1126229).

References

Bell, A.L., Brand, R.A., Pedersen, D.R., 1989. Prediction of hip joint centre location from external landmarks. Hum. Mov. Sci. 8, 3–16.

Besier, T.F., Sturnieks, D.L., Alderson, J.A., Lloyd, D.G., 2003. Repeatability of gait data using a functional hip joint centre and a mean helical knee axis. J. Biomech. 36, 1159–1168.

Besl, P.J., McKay, N.D., 1992. Year method for registration of 3-D shapes. Sensor Fusion IV: Control Paradigms and Data Structures.

Camomilla, V., Cereatti, A., Vannozzi, G., Cappozzo, A., 2006. An optimized protocol for hip joint centre determination using the functional method. J. Biomech. 39, 1096–1106.

Davis III, R.B., Ounpuu, S., Tyburski, D., Gage, J.R., 1991. A gait analysis data collection and reduction technique. Hum. Mov. Sci. 10, 575–587.

Della Croce, U., Cappozzo, A., Kerrigan, D.C., 1999. Pelvis and lower limb anatomical landmark calibration precision and its propagation to bone geometry and joint angles. Med. Biol. Eng. Comput. 37, 155–161.

Delp, S.L., Anderson, F.C., Arnold, A.S., Loan, P., Habib, A., John, C.T., Guendelman, E., Thelen, D.G., 2007. OpenSim: open-source software to create and analyze dynamic simulations of movement. IEEE Trans. Biomed. Eng. 54, 1940–1950.

Delp, S.L., Loan, J.P., Hoy, M.G., Zajac, F.E., Topp, E.L., Rosen, J.M., 1990. An interactive graphics-based model of the lower extremity to study orthopaedic surgical procedures. IEEE Trans. Biomed. Eng. 37, 757–767.

Delp, S.L., Maloney, W., 1993. Effects of hip center location on the moment-generating capacity of the muscles. J. Biomech. 26, 485–499.

Ehrig, R.M., Heller, M.O., Kratzenstein, S., Duda, G.N., Trepczynski, A., Taylor, W.R., 2011. The SCoRE residual: a quality index to assess the accuracy of joint estimations. J. Biomech. 44, 1400–1404.

Fernandez, J., Hunter, P., Shim, V., Mithraratne, K., 2012. A subject-specific framework to inform musculoskeletal modeling: outcomes from the IUPS physiome project. In: Patient-Specific Computational Modeling. Springer, pp. 39–60.

Fernandez, J., Mithraratne, P., Thrupp, S., Tawhai, M., Hunter, P., 2004. Anatomically based geometric modelling of the musculo-skeletal system and other organs. Biomech. Model. Mechanobiol. 2, 139–155.

Fiorentino, N.M., Atkins, P.R., Kutschke, M.J., Goebel, J.M., Foreman, K.B., Anderson, A.E., 2017. Soft tissue artifact causes significant errors in the calculation of joint angles and range of motion at the hip. Gait Post. 55, 184–190.

Flugsrud, G.B., Nordsletten, L., Espehaug, B., Havelin, L.I., Engeland, A., Meyer, H.E., 2006. The impact of body mass index on later total hip arthroplasty for primary osteoarthritis: a cohort study in 1.2 million persons. Arthrit. Rheumatol. 54, 802–807.

Gerus, P., Sartori, M., Besier, T.F., Fregly, B.J., Delp, S.L., Banks, S.A., Pandy, M.G., D'Lima, D.D., Lloyd, D.G., 2013. Subject-specific knee joint geometry improves predictions of medial tibiofemoral contact forces. J. Biomech. 46, 2778–2786.

Harrington, M., Zavatsky, A., Lawson, S., Yuan, Z., Theologis, T., 2007. Prediction of the hip joint centre in adults, children, and patients with cerebral palsy based on magnetic resonance imaging. J. Biomech. 40, 595–602.

Hicks, J.L., Uchida, T.K., Seth, A., Rajagopal, A., Delp, S.L., 2015. Is my model good enough? Best practices for verification and validation of musculoskeletal models and simulations of movement. J. Biomech. Eng. 137, 020905.

Kainz, H., Carty, C.P., Maine, S., Walsh, H.P., Lloyd, D.G., Modenese, L., 2017a. Effects of hip joint centre mislocation on gait kinematics of children with cerebral palsy calculated using patient-specific direct and inverse kinematic models. Gait Post. 57, 154–160.

Kainz, H., Carty, C.P., Modenese, L., Boyd, R.N., Lloyd, D.G., 2015. Estimation of the hip joint centre in human motion analysis: a systematic review. Clin. Biomech. 30, 319–329.

Kainz, H., Hajek, M., Modenese, L., Saxby, D.J., Lloyd, D.G., Carty, C.P., 2017b. Reliability of functional and predictive methods to estimate the hip joint centre in human motion analysis in healthy adults. Gait Post. 53, 179–184.

Kainz, H., Hoang, H.X., Stockton, C., Boyd, R.R., Lloyd, D.G., Carty, C.P., 2017c. Accuracy and reliability of marker-based approaches to scale the pelvis, thigh, and shank segments in musculoskeletal models. J. Appl. Biomech. 33, 354–360.

Kirkwood, R.N., Culham, E.G., Costigan, P., 1999. Radiographic and non-invasive determination of the hip joint center location: effect on hip joint moments. Clin. Biomech. 14, 227–235.

Lenaerts, G., Bartels, W., Gelaude, F., Mulier, M., Spaepen, A., Van der Perre, G., Jonkers, I., 2009. Subject-specific hip geometry and hip joint centre location affects calculated contact forces at the hip during gait. J. Biomech. 42, 1246–1251.

Lerner, Z.F., Board, W.J., Browning, R.C., 2014. Effects of an obesity-specific marker set on estimated muscle and joint forces in walking. Med. Sci. Sports Exerc. 46, 1261–1267.

Lerner, Z.F., DeMers, M.S., Delp, S.L., Browning, R.C., 2015. How tibiofemoral alignment and contact locations affect predictions of medial and lateral tibiofemoral contact forces. J. Biomech. 48, 644–650.

O'Connor, J.D., Rutherford, M., Bennett, D., Hill, J.C., Beverland, D.E., Dunne, N.J., Lennon, A.B., 2018. Long-term hip loading in unilateral total hip replacement patients is no different between limbs or compared to healthy controls at similar walking speeds. J. Biomech. 80, 8–15.

Piazza, S.J., Erdemir, A., Okita, N., Cavanagh, P.R., 2004. Assessment of the functional method of hip joint center location subject to reduced range of hip motion. J. Biomech. 37, 349–356.

Piazza, S.J., Okita, N., Cavanagh, P.R., 2001. Accuracy of the functional method of hip joint center location: effects of limited motion and varied implementation. J. Biomech. 34, 967–973.

Sangeux, M., Peters, A., Baker, R., 2011. Hip joint centre localization: evaluation on normal subjects in the context of gait analysis. Gait Post. 34, 324–328.

Sangeux, M., Pillet, H., Skalli, W., 2014. Which method of hip joint centre localisation should be used in gait analysis? Gait Post. 40, 20–25.

Schwartz, M.H., Rozumalski, A., 2005. A new method for estimating joint parameters from motion data. J. Biomech. 38, 107–116.

Seth, A., Sherman, M., Reinbolt, J.A., Delp, S.L., 2011. OpenSim: a musculoskeletal modeling and simulation framework for in silico investigations and exchange. Proc. IUTAM 2, 212–232.

Sherman, M.A., Seth, A., Delp, S.L., 2013. Year What is a moment arm? Calculating muscle effectiveness in biomechanical models using generalized coordinates. ASME 2013 International Design Engineering Technical Conferences and Computers and Information in Engineering Conference.

Winter, D.A., 1989. Biomechanics of normal and pathological gait: implications for understanding human locomotor control. J. Mot. Behav. 21, 337–355.
Wu, G., Siegler, S., Allard, P., Kirtley, C., Leardini, A., Rosenbaum, D., Whittle, M., D D'Lima, D., Cristofolini, L., Witte, H., 2002. ISB recommendation on definitions of joint coordinate system of various joints for the reporting of human joint motion—Part I: ankle, hip, and spine. J. Biomech. 35, 543–548.
Zeni, J., Pozzi, F., Abujaber, S., Miller, L., 2015. Relationship between physical impairments and movement patterns during gait in patients with end-stage hip osteoarthritis. J. Orthop. Res. 33, 382–389.
Zhang, J., Fernandez, J., Hislop-Jambrich, J., Besier, T.F., 2016. Lower limb estimation from sparse landmarks using an articulated shape model. J. Biomech. 49, 3875–3881.
Zhang, J., Malcolm, D., Hislop-Jambrich, J., Thomas, C.D.L., Nielsen, P.M., 2014a. An anatomical region-based statistical shape model of the human femur. Comput. Meth. Biomech. Biomed. Eng. Imag. Visual. 2, 176–185.
Zhang, J., Sorby, H., Clement, J., Thomas, C.D.L., Hunter, P., Nielsen, P., Lloyd, D., Taylor, M., Besier, T., 2014b. Year The MAP client: user-friendly musculoskeletal modelling workflows. International Symposium on Biomedical Simulation.